REPORT DOCUMENTATION PAGE

Public reporting burden for this collection of information is estimated to average 1 hour per response, including the time for reviewing instructions, searching existing data sources, gathering and maintaining the data needed, and completing and reviewing the collection of information. Send comments regarding this burden estimate or any other aspect of this collection of information, including suggestions for reducing this burden, to Washington Headquarters Services, Directorate for Information Operations and Reports, 1215 Jefferson Davis Highway, Suite 1204, Arlington, VA 22202-4302, and to the Office of Management and Budget, Paperwork Reduction Project (0704-0188), Washington, DC 20503

1. AGENCY USE ONLY (Leave blank)	2. REPORT DATE 10/16/97	3. REPORT TYPE AND DATES COVERED Technical Report, May 96 - Sept. 97

4. TITLE AND SUBTITLE
Thin Layer Electrochemical Studies of ZnS, ZnSe, and ZnTe Formation by Electrochemical Atomic Layer Epitaxy (ECALE)

5. FUNDING NUMBERS
G-N00014-19-J-1919
96 Pro - 2855
R&T 4133036

6. AUTHOR(S)
Lisa P. Colletti, Sajan Thomas, Elvin Wilmer, and John L. Stickney

7. PERFORMING ORGANIZATION NAME(S) AND ADDRESS(ES)
Department of Chemistry
University of Georgia
Athens, GA 30602-2556

8. PERFORMING ORGANIZATION REPORT NUMBER
Technical Report #28

9. SPONSORING / MONITORING AGENCY NAME(S) AND ADDRESS(ES)
Office of Naval Research
Chemistry Division
800 North Quincy Street
Arlington, VA 22217-5660

10. SPONSORING / MONITORING AGENCY REPORT NUMBER

11. SUPPLEMENTARY NOTES

12a. DISTRIBUTION / AVAILABILITY STATEMENT
Approved for public release and sale: its distribution is unlimited

12b. DISTRIBUTION CODE

13. ABSTRACT (Maximum 200 words)

Thin-layer electrochemical studies of the underpotential deposition (UPD) of Zn, Te, Se, and S on polycrystalline Au substrates have been performed. These studies were initiated to investigate the electrodeposition of ZnTe, ZnSe, and ZnS by electrochemical ALE (ECALE). Zn UPD on Au begins at -0.5 V and results in a coverage of 0.47 monolayer (ML). Te and Se atomic layers were formed using a two step process were bulb chalcogenide was removed by reduction, leaving the atomic layer. The reduction of the last atomic layer of Te or Se was not observed, regardless of how negative the potential was scanned. Sulfur atomic layers were spontaneously deposited below -0.6 V from a sulfide solution. Thermodynamic effects are clearly evident during the first monolayer of deposition. Zinc deposition onto Te, Se, and S coated electrodes occurs at progressively more positive potentials as the stability of the zinc compounds increase.

This initial information was used to develop ECALE cycles for the compounds, and thin-films were formed by repeated application of the cycles. The dependence of the deposit coverage on the deposition potentials was examined and found to display the characteristic "S" curve of a surface limited process. In addition, the dependence of the coverage on the number of ECALE cycles performed was found to be near the ideal 0.5 ML per cycle for ZnSe and ZnS. The ZnTe coverage per-cycle was less-than expected indicating that further optimization of deposition conditions is needed.

14. SUBJECT TERMS
Electrodeposition, underpotential deposition, atomic layer epitaxy, ALE, ZnTe, ZnSe, ZnS

15. NUMBER OF PAGES 10

16. PRICE CODE

17. SECURITY CLASSIFICATION OF REPORT	18. SECURITY CLASSIFICATION OF THIS PAGE	19. SECURITY CLASSIFICATION OF ABSTRACT	20. LIMITATION OF ABSTRACT
Unclassified	Unclassified	Unclassified	UL

Thin Layer Electrochemical Studies of ZnS, ZnSe, and ZnTe Formation by Electrochemical Atomic Layer
Epitaxy (ECALE)

By
Lisa P. Colletti, Sajan Thomas, Elvin Wilmer, and John L. Stickney

Department of Chemistry
University of Georgia
Athens, GA 30602-2556

October 15, 1997

19971028 167

Thin Layer Electrochemical Studies of ZnS, ZnSe, and ZnTe Formation by Electrochemical Atomic Layer Epitaxy (ECALE)

Lisa P. Colletti, Sajan Thomas, Elvin M. Wilmer, and John L. Stickney*
Department of Chemistry, University of Georgia, Athens, Ga. 30602

Abstract

Thin-layer electrochemical studies of the underpotential deposition (UPD) of Zn, Te, Se, and S on polycrystalline Au substrates have been performed. These studies were initiated to investigate the electrodeposition of ZnTe, ZnSe, and ZnS by electrochemical ALE (ECALE). Zn UPD on Au begins at -0.5 V and results in a coverage of 0.47 monolayer (ML). Te and Se atomic layers were formed using a two step process where bulk chalcogenide was removed by reduction, leaving the atomic layer. The reduction of the last atomic layer of Te or Se was not observed, regardless of how negative the potential was scanned. Sulfur atomic layers were spontaneously deposited below -0.6 V from a sulfide solution. Thermodynamic effects are clearly evident during the first monolayer of deposition. Zinc deposition onto Te, Se, and S coated electrodes occurs at progressively more positive potentials as the stability of the zinc compounds increase.

This initial information was used to develop ECALE cycles for the compounds, and thin-films were formed by repeated application of the cycles. The dependence of the deposit coverage on the deposition potentials was examined and found to display the characteristic "S" curve of a surface limited process. In addition, the dependence of the coverage on the number of ECALE cycles performed was found to be near the ideal 0.5 ML per cycle for ZnSe and ZnS. The ZnTe coverage per cycle was less than expected indicating that further optimization of deposition conditions is needed.

Introduction

Compound semiconductor thin-film formation via electrodeposition may some day prove to be a simple, cost effective method relative to chemical vapor deposition (CVD) or molecular beam epitaxy (MBE). Possible advantages of an electrochemical deposition technique include deposition at or near equilibrium, a low deposition temperature, and the ability to deposit uniform films on large and irregularly shaped objects. In addition, environmental concerns over toxic organometallic chemicals are eliminated or reduced with the use of dilute aqueous solutions of ionic reactants [1]. A significant number of electrodeposition studies of II-VI compound semiconductors have been performed previously, primarily involving formation of the Cd based compounds, given their applicability to solar energy conversion. However, interest in zinc based II-VI compounds is increasing due to their use in phosphors, thin-film electroluminescent displays [2], and emerging optoelectronic technologies [3,4]. ZnSe, in particular, is being extensively studied due to applications such as solid state blue lasers and blue light emitting diodes [4].

Electrodeposition of the zinc based II-VI compounds has predominantly involved aqueous codeposition techniques to form zinc telluride [5], zinc selenide [6-14], and zinc sulfide [15-17] thin-films. X-ray diffraction (XRD) analysis [12,14-16] has shown the electrodeposited zinc chalcogenide films to be polycrystalline, while scanning electron microscopy (SEM) has shown discontinuous [16] or grainy films [5,12,15,17]. So far, only one study of ZnTe codeposition appears to have been reported [5]. Those were able to find conditions from which stoichiometric films could be formed; however, annealing was required to improve the optical properties of the film. Of the many ZnSe studies, two [12,14] have involved characterization of their films using techniques other than photoelectrochemistry. Natarajan et al. [12] concluded that an excess of Se in the films was unavoidable due to the complicated chemistry of Se. Vacuum annealing was required to produce stoichiometric ZnSe films. In contrast, Ohno et al. [14] found deposition conditions which formed stoichiometric ZnSe without annealing. For ZnS films, only Sanders and Kitai [16] determined the elemental stoichiometry. Auger spectroscopy analysis showed stoichiometric Zn:S ratios.

Work in our group presently involves development of an alternative electrochemical deposition technique, electrochemical ALE (ECALE) [18,19], the electrochemical analog of atomic layer epitaxy (ALE) [20-22]. In traditional vacuum-based ALE, control over deposit structure and stoichiometry is achieved using a cycle of surface limited reactions, to deposit atomic layers of the individual elements. In ECALE, underpotential deposition (UPD) [23], another name for a surface limited reaction, is used to deposit atomic layers of each element, again in a cycle.. To form thin films, the cycle is repeated until the desired thickness is reached.

It appears that significantly more control is achieved over the deposition process using electrochemical ALE then with other electrodeposition methods. Ideally, stoichiometric and crystalline deposits will be formed without the need for post deposition heat treatments using EACLE. The present paper describes a series of studies performed to delineate conditions for the growth of Zn based II-VI compounds. The conditions determined here

then serve as a first approximation of those needed for the automated electrodeposition of zinc chalcogenide thin films [24,25].

Experimental

, Studies were performed in a static thin layer electrochemical cell (TLEC), described in detail elsewhere [18,26]. The TLEC consisted of an polished, annealed, polycrystalline Au cylinder in a fitted glass cavity with a solution gap of about 0.03 mm. Two holes were provided at the bottom (tip) of the TLEC to allow solution into and out of the cavity and for ionic conductivity. Solution aliquots were drawn in by capillary action and expelled by pressurizing the cell interior with N_2 gas. The process of blowing out one aliquot of solution out and allowing another to wick in, is referred to as a rinse.

Other hardware consisted of a series of Pyrex glass "H-cells" that consist of two compartments divided by a fine glass frit [18]. N_2 gas was used to sparge all solutions prior to each experiment. Separate H-cells were used for each solution and the TLEC was carefully transferred between them for access to a given solution. The potentiostat was built in-house with a conventional op-amp based design. The reference electrode was Ag/AgCl, made with 1.0 M NaCl, and the auxiliary electrode was a Au wire. All solutions were made with 18 M-ohm water from a Nanopure water filtration system, fed from the house deionized water system. All experiments were performed at room temperature.

To assure surface cleanliness, each electrochemical experiment was preceded by at least three electrochemical cleaning cycles; each cycle consisted of ten rinses with fresh 1M H_2SO_4 at 1.4 V, followed by 10 rinses at -0.5 V. A cyclic voltammogram, taken after three cleaning cycles, was used as a check of surface cleanliness (Figure 1A).

Experimental coverages are reported as the ratio of deposited atoms per substrate surface atom. A 1.2 cm^2 geometric surface area was determined and a roughness factor of 1.2 was assumed. A coverage of 1.17 x 10^{15} Au atoms/cm^2 was used, corresponding to a Au(100) surface. The coverage of a Au(100) surface is intermediate between those of the other two low-index planes: 1.35 x 10^{15} atoms/cm^2 for Au(111) and 8.2 x 10^{14} atoms/cm^2 for Au(110). The assumption here is that a polycrystalline electrode can be represented as some average of all three low index planes.

Potential (V vs. Ag/AgCl)

Figure 1: Cyclic voltammetry of a polycrystalline Au electrode in a thin-layer cell: (A) clean Au electrode in 1 M H_2SO_4; (B) clean Au electrode in 0.5 M $NaClO_4$ + 0.05 M $HOCOC_6H_4COOK$ (KHP), pH 5.7; (C) clean Au electrode in 10 mM $ZnSO_4$ + 5 M $NaClO_4$ + 0.05 M KHP, pH =5.7; (D) Zn alloyed Au electrode in 1 M H_2SO_4 after three cleaning cycles with an oxidation potential of 1.3 V. All scans were taken at 5 mVs^{-1}.

Results and Discussion

Zn Deposition

Zn electrodeposition on Ag [27], Au [28-31], and Pt [29,31-35] has been extensively investigated on both polycrystalline and single crystalline substrates. It is a complex system, consisting of an initial UPD process, alloy formation, and bulk deposition. To complicate matters, there are indications, via X-ray absorption spectroscopy (XAS), that alloying occurs between Au and Zn even within the UPD region [30].

A cyclic voltammogram of the clean gold electrode in the zinc blank solution, pH 5.7, is shown in Figure 1B. Gold oxidation begins above 0.8 V, with the corresponding gold reduction at 0.75 V. Hydrogen evolution slowly begins below -0.4 V. In Figure 1C, one aliquot of a $ZnSO_4$ solution was rinsed into the TLE under open
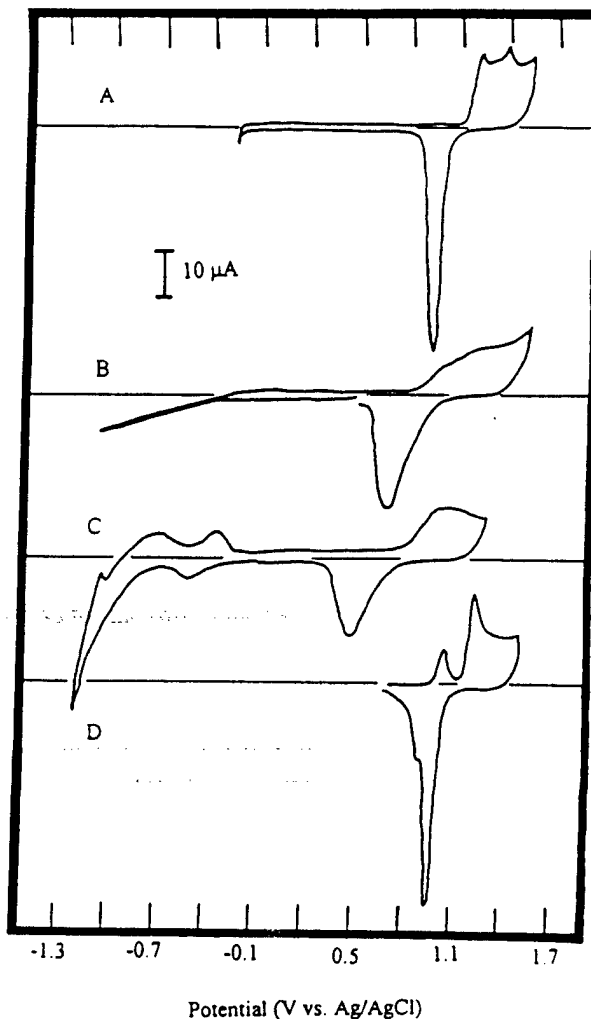
2

circuit conditions and subsequently scanned negatively from the rest potential, - 0.11 V. A small reductive Zn UPD peak is evident at -0.5 V resulting in a coverage of 0.47 monolayer (ML). Below -0.9 V, the reductive current begins to increase slowly, and on the subsequent positive going scan displays a small spike near -1.1 V. This small spike corresponds to bulk Zn stripping, indicating the formal potential for the Zn^{2+}/Zn couple in this solution is near -1.1 V. In addition to the currents for UPD and bulk deposition there appears to be other charge passed. For example, the net current at potentials bellow -0.9 V is cathodic, even on the positive going sweep. This could be attributed to hydrogen evolution, such as is evident in Figure 1B. However, there appears to be more current then expected on the negative going scan between -0.7 V and -1.1 V, possibly the result of a decreased hydrogen overpotential on the Zn modified surface. Alternatively, this current may be associated with the deposition of Zn, as there is a corresponding stripping feature between -1.0 V and -0.5 V, and hydrogen cannot be oxidized at these potentials. It is more likely that this extra charge is the formation of a Zn-Au alloy, as previously suggested by other workers [28-30]. Further evidence of alloying was observed during the subsequent cleaning procedure. When potentials less than 1.4 V were used as the positive limit in cleaning cycles, residual amounts of a Zn-Au alloy appeared to be present; indicated by a new feature at 0.95 V (Figure 1D) compared to the clean surface voltammetry (Figure 1A). A report by Tadjeddine and Torillon [30] supports this conclusion, as they found interactions between the zinc and gold in the alloy were so strong that high anodic potentials were required to oxidize the alloyed zinc. Finally, the UPD stripping feature is evident at -0.3 V, and is slightly larger (0.5 ML) then the corresponding deposition peak, which is understandable considering that it is probably superimposed on some of the Zn-Au alloy stripping current. Similar behavior appears to take place in the Cd-Au system [36,37].

Chalcogenide deposition

Figure 2 shows a series of thin-layer voltammograms for deposition of the chalcogenides on polycrystalline Au. Ideally, the chalcogenide atomic layers in an ECALE cycle would be formed directly by oxidative UPD, using a solution containing the element in a -2 oxidation state: Te^{2-}, Se^{2-}, or S^{2-}. Unfortunately aqueous solutions of both Te^{2-} and Se^{2-} tend to be unstable; therefore, $HTeO_2^+$ and $HSeO_3^-$ solutions have been used as chalcogenide sources. Prior to each deposition, a clean voltammogram was obtained, similar to that shown in Figure 1A.

The clean TLEC was then immersed into the chosen chalcogenide solution and an aliquot rinsed in. Figure 2A is for an aliquot of $HTeO_2^+$ solution. Two reversible couples at 0.20 V and 0.10 V correspond to Te UPD and bulk Te deposition, respectively. The bulk deposition feature is smaller than the UPD, since the amount of $HTeO_2^+$ present in the aliquot was limited. The small bulk peak represents deposition of all the Te not already deposited during the UPD process. The peaks are fairly broad for several reasons. One is that the cleaning procedure consists of a sequence of oxidation and reduction cycles that can result in surface roughening of an already polycrystalline Au electrode [38-41]. In addition, the peaks are broadened by changes in the $HTeO_2^+$ activity while the deposition is proceeding. There are also problems with IR drop due to the thin layer configuration. At potentials just below -1.0 V, another reversible couple is visible, corresponding to the reduction of bulk Te to Te^{2-}.
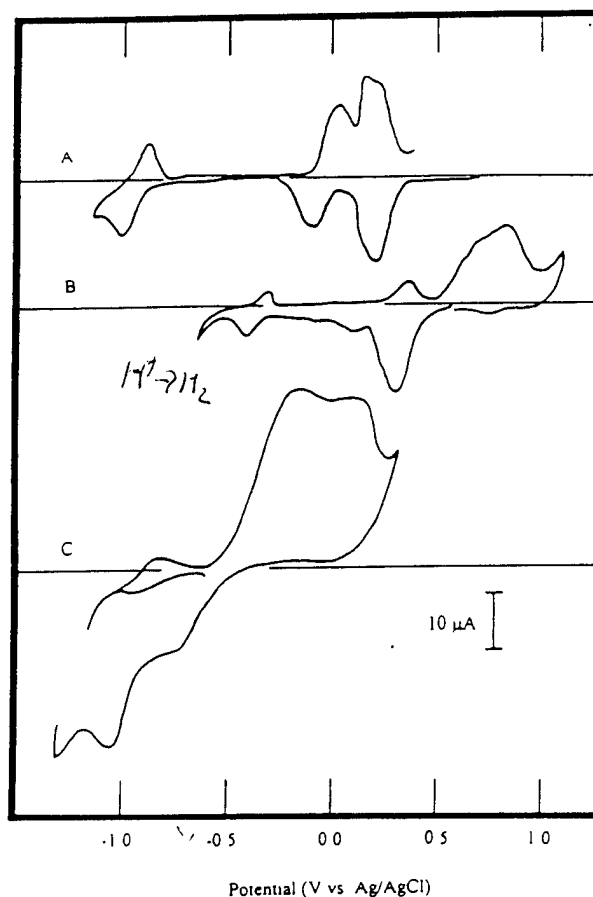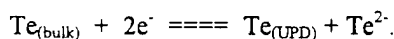
$$Te_{(bulk)} + 2e^- ==== Te_{(UPD)} + Te^{2-}. \qquad \{1\}$$

Figure 2: Cyclic voltammetry of the chalcogenides in a thin-layer cell: (A) clean Au electrode in 0.25 mM TeO_2 + 0.5 M Na_2SO_4 + 0.01M $Na_2B_4O_7$, pH 9.2; (B) clean Au electrode in 1.0 mM SeO_2 + 0.5 M $NaClO_4$ + 0.01M $Na_2B_4O_7$, pH 8.6; (C) clean Au electrode in 2.5 mM Na_2S + 0.5 M $NaClO_4$, pH 11.7. All scans were taken at 5 mVs^{-1}.

As these experiments were performed with a traped solution volume, in a TLEC, any Te^{2-} formed stayed in the cell and could be quantitatively reoxidize to Te during the anodic scan.

Figure 2B is a voltammogram for the corresponding deposition of Se from a solution of $HSeO_3^-$. The voltammograms in Figures 2A and B are very similar, with the main difference being the potentials needed to reduce bulk Se to Se^{2-} versus bulk Te to Te^{2-}. Selenium reduction occurs several hundred milivolts positive of the corresponding Te reduction feature. No features were observed for the reduction of UPD Se or Te, regardless of how negative the potential was scanned.

An atomic layer of Te or Se can be formed if the TLE is rinsed with pure supporting electrolyte after the UPD peak, at 0.05 V or at 0.14 V respectively. Alternatively, the whole aliquot can first be deposited, followed by the reaction in eq. 1 where excess Te or Se is reduced from the surface and rinsed away. While depositing a Te or Se UPD layer by the first method is relatively straight forward, it cannot be used in the formation of a second layer of a Zn chalcogenide. Zinc is clearly not stable on the surface at such potentials. Thus, the second, two step method, based on eq. 1, must be used for all but the first atomic layer of Te or Se.

Sulfide solutions are relatively stable compared with telluride and selenide solutions; thus, UPD of a S atomic layer is a more direct process. Figure 2C is the voltammetry of an aliquot of a sodium sulfide solution. It starts with a negative scan from -0.6 V to -1.2 V, displaying reductive stripping of a spontaneously formed S UPD layer [37,42-44]. Reversal of the scan at -1.2 V shows the UPD peak at -0.85 V. Continuation of the scan to 0.30 V reveals a very large peak, corresponding to oxidation of the remaining S^{2-} to bulk S. At 0.3 V, the current begins to increase again, as the deposited S starts to convert to sulfate [37]. A second reversal at this point, resulted in no current flow until -0.6 V, after which, reduction of sulfur to polysulfide occurred [37]. Below -1.2 V, solvent decomposition was the dominant process.

Zn Chalcogenide Formation

Figure 3 is a series of diagrams showing the deposition of Zn on atomic layers of Te, Se, and S. Comparing the voltammetry, there is a definite trend going up the periodic table. Zn is hardest to deposit on the Te atomic layer, not starting till -0.7 V. A well defined Zn UPD peak is visible for the Se atomic layer, beginning at -0.5 V. Finally, deposition of Zn on the S atomic layer begins near -0.3 V. The differences in the UPD potentials are consistent with differences in the free energies of formation of the compounds: -115.2, -173.6, -200.0 kJ/mol for ZnTe, ZnSe, and ZnS respectively [45].

The rest of this article describes TLEC studies of Zn chalcogenide electrodeposits. Each experiment involved formation of a deposit under a specific set of cycle conditions for a specified number of cycles. Coulometric stripping was then used to characterize elemental coverages per cycle as a function of the deposition potentials. These experiments proved very tedious but worthwhile. If 10 cycles were to be deposited under a specific set of conditions, then extreme care had to be taken as there were a minimum of 12 steps per cycle (Figure 4). Note that for the ECALE cycle diagrammed in Figure 4, each solution was in a separate H-cell. The TLEC, reference, and auxiliary electrodes were moved from H-cell to H-cell at each step. To prevent cross contamination of the separate solutions and the Au electrode, the TLEC exterior was rinsed with H_2O

Figure 3: Cyclic voltammetry of an aliquot of 10 mM $ZnSO_4$: (A) with a Te coated electrode; (B) with a Se coated electrode; (C) with a S coated electrode.

while pressurized with N_2 (shown in Figure 4 as an H_2O solution block). Each cycle started with three rinses in the S blank at -1.0 V. This was done to condition the TLE, as the glass walls act as a reservoir for H^+ ions from the more acidic Zn solutions. Then two aliquots of S were rinsed in at -1.0V. Before blowing out the second aliquot, the electrode was held at this potential for 30 seconds to deposit the S UPD layer. This was followed by
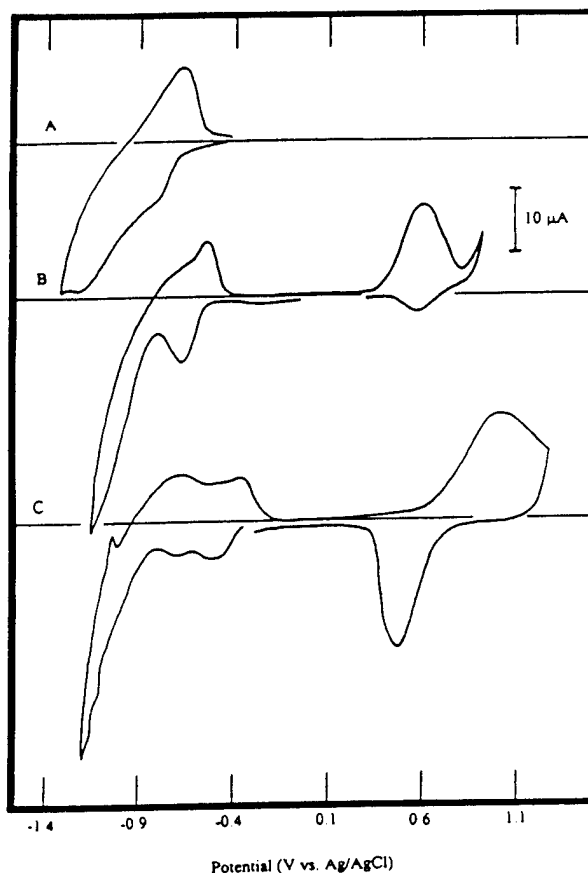
Figure 4: Diagram of the sequence of steps used in an one complete ZnS ECALE cycle. See text for details
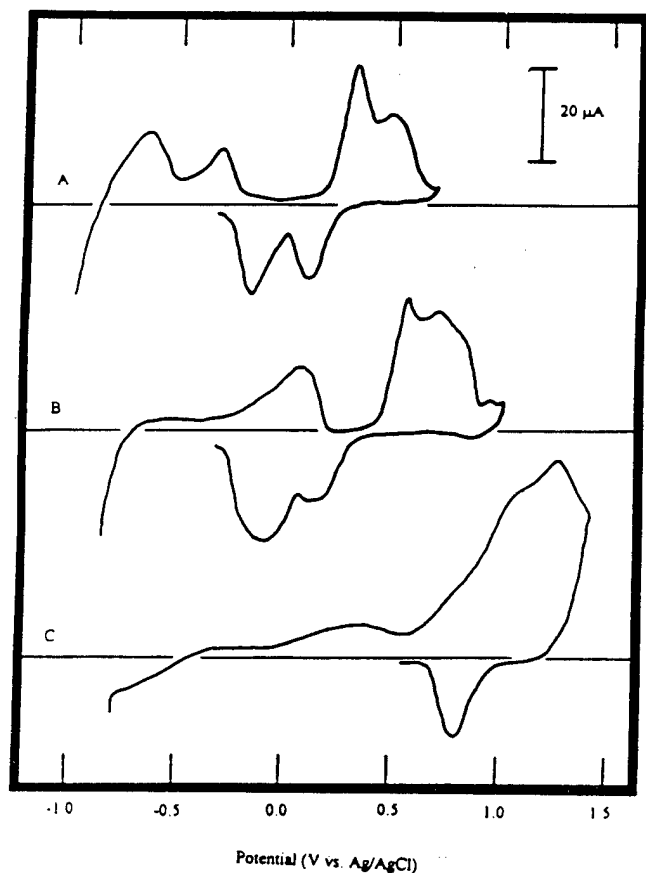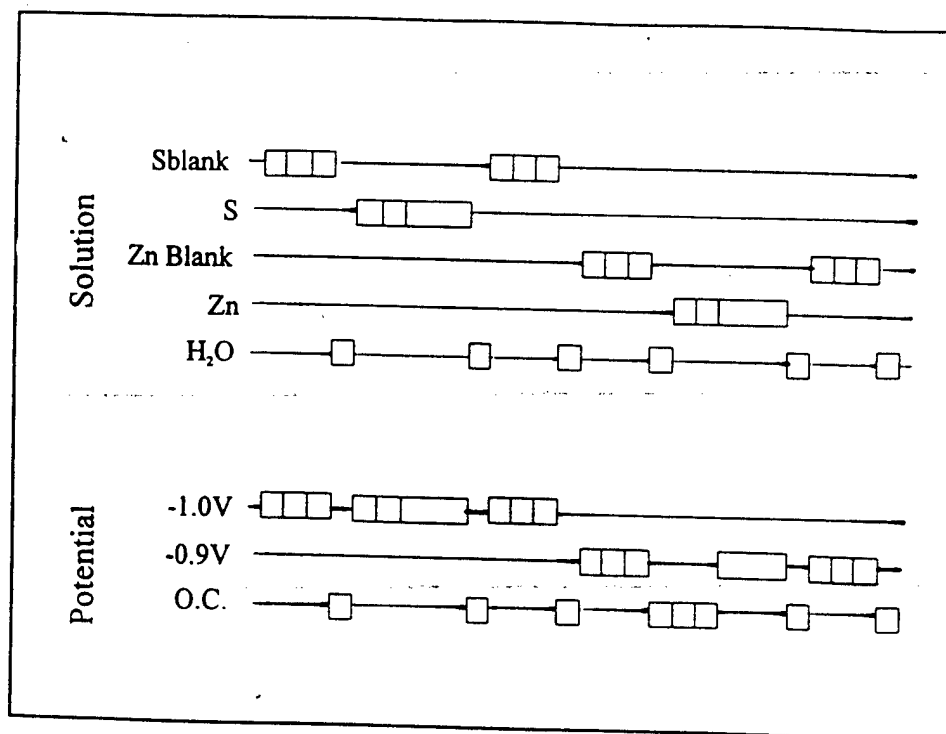

Figure 5: Stripping voltammetry taken at 5 mVs^{-1} of 4 ECALE cycles: (A) ZnTe in 0.5 M Na$_2$SO$_4$, pH 3; B) ZnSe 0.5 M NaClO$_4$, pH 3; C) ZnS in 0.5 M NaClO$_4$, pH 3.
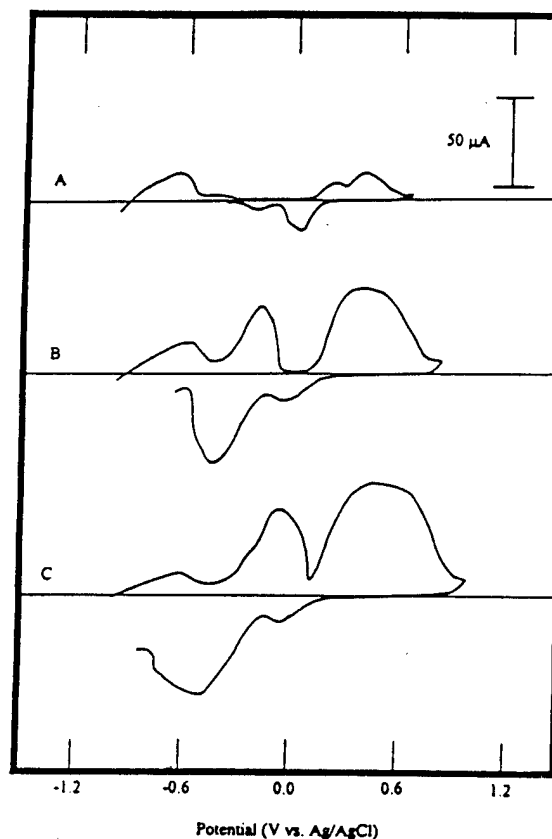
Figure 6: Stripping voltammetry taken at 5 mVs^{-1} of ZnTe in 0.5M Na$_2$SO$_4$, pH 3: (A) 2 ECALE cycles; (B) 8 ECALE cycles; (C) 16 ECALE cycles.

5

three more rinses in the S blank at -1.0 V to remove any excess S species. The electrode was then removed, rinsed, and placed into the Zn blank solution at -0.9 V where three rinses were performed, conditioning the TLE for the more acidic environment. This was followed by two open circuit rinses of the Zn solution with the second aliquot of Zn held at -0.9 V to deposit a UPD layer. Three more rinses with the Zn blank were performed to remove any remaining Zn^{2+} ions.

Figure 5 consists of stripping curves for deposits resulting from four ECALE cycles of ZnTe (A), ZnSe (B), and ZnS (C). Several trends are evident. First, a trend similar to that seen during deposition of the initial Zn atomic layer (Figure 3) is observed: the Zn was easier to strip from the ZnTe then from ZnSe then from ZnS. From Figure 5, it also appears that there are generally two Zn stripping features in each scan. This is seen most demonstratively for ZnTe in Figure 5A, where the low potential peak, -0.7 V, grows in first but does not significantly increase in size after the second cycle (Figure 6). Instead the higher potential feature, -0.3 V, starts to grow. As the number of cycles is increased further, this second peak grows and shifts to still higher potentials. A simple explanation would be that the first peak represents the top layer of Zn atoms, those not completely coordinated to Te, while the second peak represents Zn from the interior of the compound.

In the next series of graphs, the number of monolayers of the elements deposited per cycle has been plotted as a function of the potential used to deposit one of the elements. The coverages should not be taken too literally at this stage. Theoretically, a coverage of 0.5 ML of each element per cycle should be optimal, as it takes 0.5 ML of each element to form 1 ML of the compound. However, the coverage measurements are made with a number of assumptions including the number of Au surface atoms and the background correction used in the coulometry.

Determination of the potentials needed to deposit atomic layers of Te and Se was straight forward. As mentioned above, they are formed by first depositing a few monolayers of the element and then reducing the surface at fairly negative potentials to remove the excess. The potentials at which Te and Se reduce are below -1.0 V for Te, and below -0.5 V for Se. Reduction of the last atomic layer of the chalcogenide was very difficult to achieve, as hydrogen evolution polarized the electrode potential, and obscured the reduction process before the atomic layers could be removed. Thus, any potential below -1.0 V for Te, or below -0.5 V for Se, should work for forming atomic layers.

The choice of conditions for formation of S atomic layers from sulfide solutions was less clear cut. Figure 7 is a graph of the monolayer/cycle for deposits formed after 3 cycles, as a function of the S deposition potential. The Zn deposition potential was -0.9 V for these studies. The resulting graphs of S and Zn coverage do not coincide well. Possible explanations include a problem in quantifying the voltammograms. In Figure 5, the Zn stripping feature overlaps significantly with the S oxidation feature after only four cycles. Regardless of the discrepancy between the Zn and S coverages, the trends appear valid.

ALE behavior is frequently indicated by an "S" curve. That is, for a given variable, at one extreme the coverage is too high, while at the other the coverage is too low. In between, there is a plateau, where deposition is controlled by surface limited reactions alone, and one monolayer of the compound is formed per cycle [20-22]. In Figure 7, at the most negative S deposition potentials, below -1.1 V, insufficient S is deposited each cycle, and since Zn requires the presence of S, both coverages drop. At potentials above -0.9 V, both coverages increase, as bulk S begins to be incorporated into the deposits. That increase, however, starts to drop off at potentials above -0.7 V, as Zn no longer remains on the surface during the S deposition step. The

Figure 7: Graph of the coverages of Zn (□) and S (Δ) per ECALE cycle as a function of the potential used for S deposition.

conclusion drawn from this study is that S should be deposited at potentials between -1.1 V and -0.9 V, where there is a small plateau, indicating probable surface limited control over the deposition.
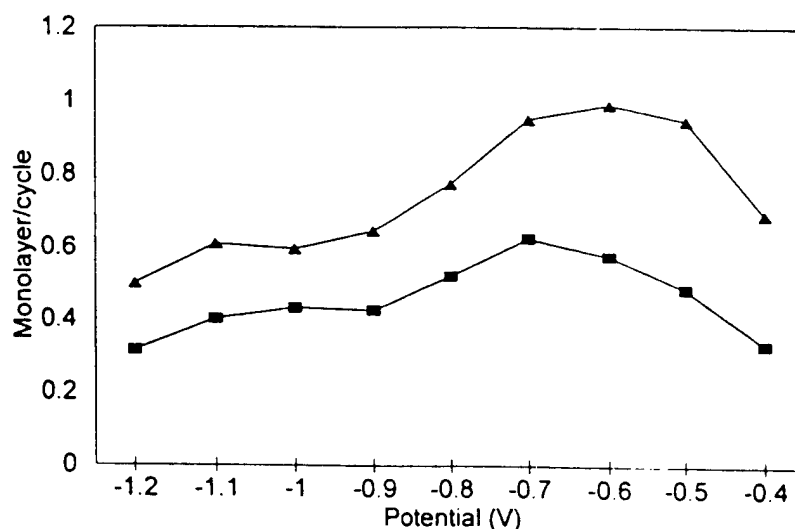
From Figure 7, it was decided to proceed using -1.0 V for the deposition of S atomic layers. Figure 8 is then a graph of the coverages of Zn and S as a function of the Zn deposition potential, holding S deposition at -1.0 V. The dependence on the Zn potential is not dramatic, with only small changes in coverage/cycle as the potential is varied from -1.0 V to -0.5 V. As mentioned, -0.9 V was used as the Zn deposition potential in the studies shown in Figure 7. The difference in coverage between Zn and S are significant at -0.9 V and above in Figure 8, as they were in Figure 7. At -1.2 V, the Zn coverage is increasing, as bulk Zn deposition becomes important. At potentials more positive than -0.5 V, not enough Zn is being deposited and the coverages of both elements drop. The underpotential for Zn deposition appears to be negative of -0.5 V. A Zn deposition potential of -1.0 V appears optimal, as the coverages coincide well and are very close to the ideal 0.5 ML per cycle for each element. For this compound a cycle where both elements are deposited at -1.0 V looks to be the best starting point for further studies of ZnS deposition by ECALE.

Figure 9 is a similar graph of coverage/cycle, for the deposition of ZnSe as a function of the Zn deposition potential. Selenium deposition was carried out by first depositing several monolayers at -0.9 V, and then reducing off any excess at -0.9 V. The drop in the coverages above -0.8 V is due to decreasing Zn stability. A plateau in both the Zn and Se coverages is evident between -1.2 V and -0.9 V; however, it corresponds to Zn coverage/cycle of nearly 0.75 ML, while the Se coverage remains at 0.5 ML. Given the data in Figure 9, however, the optimal Zn potential appears to be between -0.9 V and -0.7 V, with -0.8 V looking best.

Figure 10 is the corresponding graph of coverage/cycle as a function of the Zn deposition potential in the formation of ZnTe. The Te was deposited by first forming a couple of monolayers at -0.8 V, and then reductively stripping the excess at -1.1 V. Under the conditions chosen, the Te coverage/cycle looks low at all potentials, about 0.33 ML per cycle. This is not the expected behavior, and indicates that the dependence of Te coverage on its deposition conditions needs more study. There is a plateau between -1.1 V and -1.0 V, similar to that seen in Figure 9
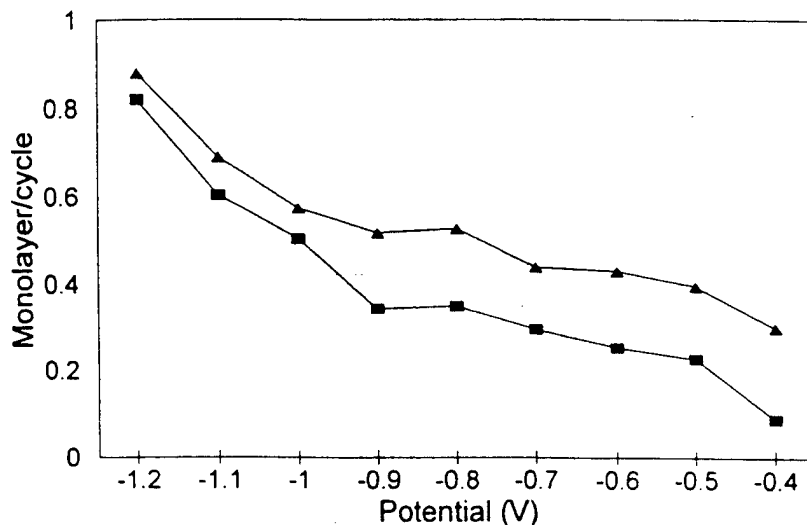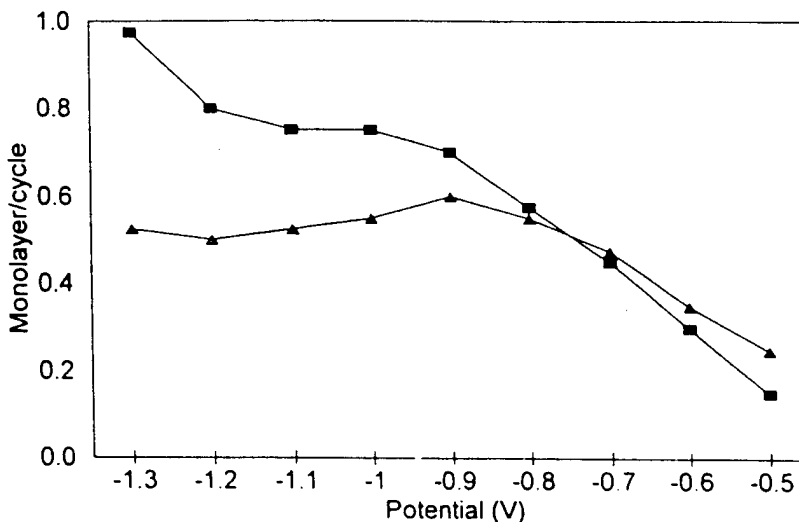

Figure 8: Graph of the coverages of Zn (□) and S (Δ) per ECALE cycle as a function of the potential used for Zn deposition.

Figure 9: Graph of the coverages of Zn (□) and Se (Δ) per ECALE cycle as a function of the potential used for Zn deposition.
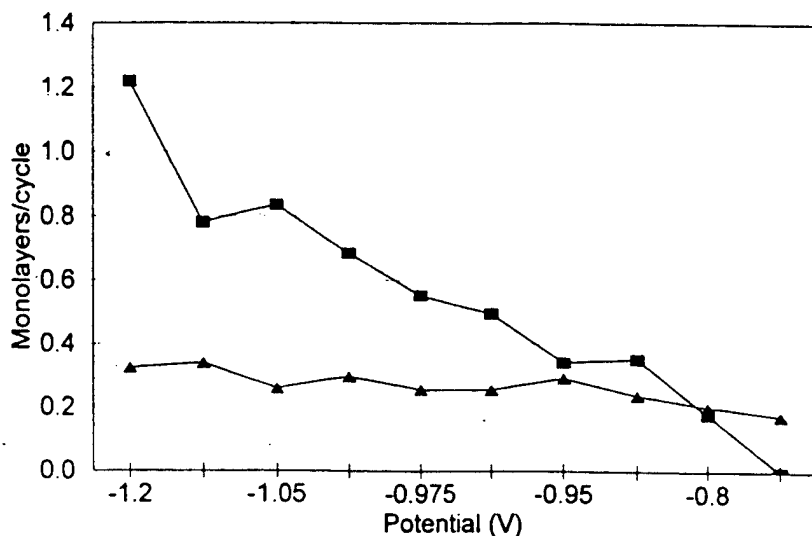
for ZnSe formation, where the Zn coverage is significantly higher than the corresponding chalcongenide, again. It is not clear what is causing this, besides maybe alloy formation between the Zn and Au [28-30]. Between -0.95 V and -0.8 V the coverages/cycle for Zn and Te coincide and correspond to about 0.33 ML/cycle. Positive of -0.8 V, the coverage of Zn falls off quickly, as expected. Given the data presented in Figure 10, a Zn deposition potential of -0.95 V would probably be optimal.

Figure 10: Graph of the coverages of Zn (□) and Te (Δ) per ECALE cycle as a function of the potential used for Zn deposition.

Finally, given the starting conditions determined from Figures 7-10, studies were performed investigating the dependence of the coverage on the number of cycles performed (Figure 11). A linear dependence is expected for an ALE process, and is evidenced in each of the graphs in Figure 11, given the error inherent in the measurements. The slopes in the case of ZnSe and ZnS formation are very close to the expected 0.5 ML per cycle. The slope is a little low in the case of ZnTe, in line with the need to better optimize the Te deposition. In all three graphs, there is a drop off in the coverages, at the highest number of cycles. This may be a quantitation problem as the stripping peaks for the two elements start to overlap. In the present studies, clear problems were encountered after 16 cycles of ZnTe, 10 cycles of ZnSe, and only 4 cycles of ZnS, due to broadening of the Zn stripping peaks at higher potentials, as the coverage increases. They eventually run into the chalcogenide stripping features (e.g. Figure 5C), making it difficult to independently determine the coverages of the two elements. It may also be a problem with operator error, as each cycle involves 24 or more steps; therefor, as the number of cycles increase, there are more chances for mistakes, suggesting that the next step should be to use an automated system [24,25].

Conclusion

Thin layer electrochemical cells have been used to study the conditions needed to deposit Zn chalcogenides by electrochemical ALE. It is fortuitous that the stripping voltammetry of deposited layers can be used to determine the coverages of both elements in the compound; however, it is limited to the first few cycles where the stripping features do not overlap. The studies presented here demonstrate behavior consistent with an ALE process. That is, deposit coverages increase linearly with the number of cycles, 0.5 ML deposits of each element are formed each cycle, and the characteristic "S" curve dependence of deposit coverages with various cycle variables are observed.

There are obvious discrepancies in the data presented. The sources are not all clear, however they do provide a good starting point for further studies. An automated deposition system has been constructed and will be used in subsequent studies. It will provide more reproducible results, and allow the formation of thicker deposits which can be studied using techniques such as electron probe microanalysis (EPMA) and X-ray diffraction (XRD). This will provide a better environment for optimization of deposition parameters.
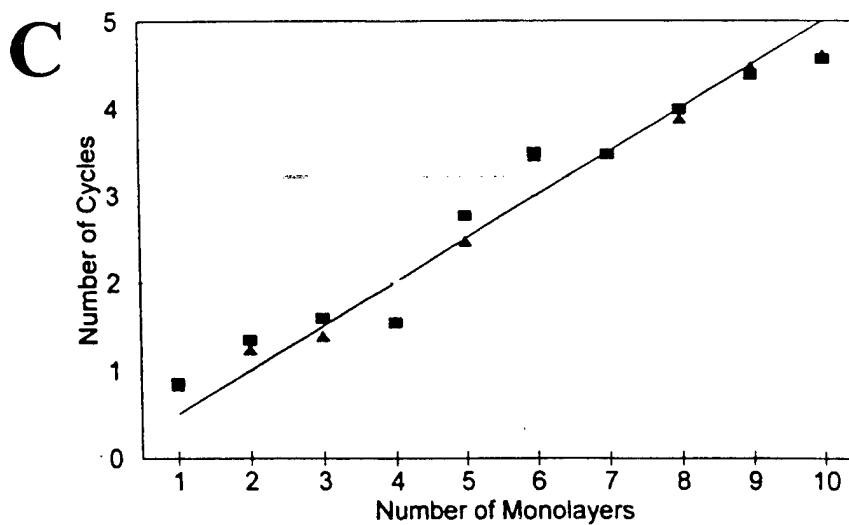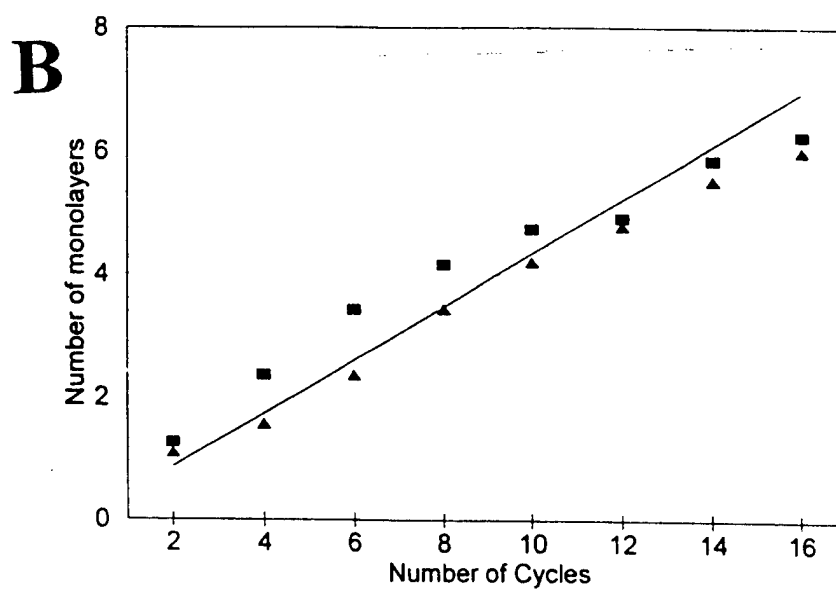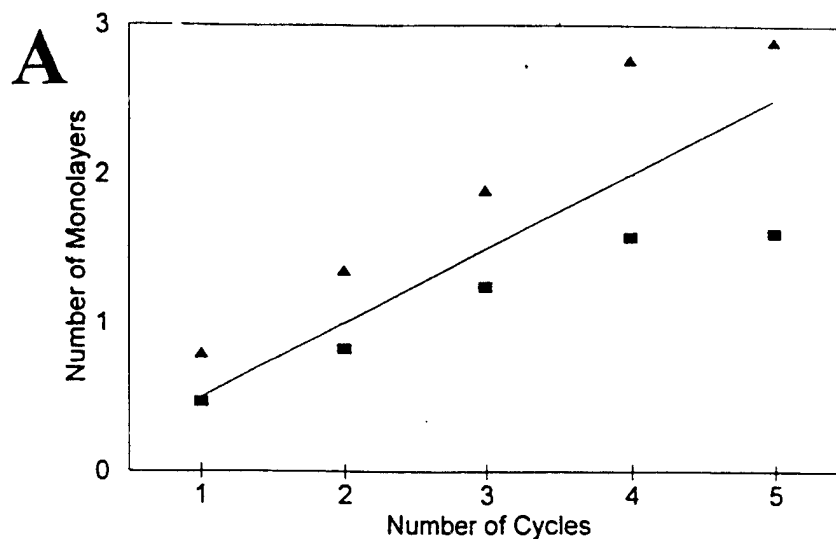
Acknowledgments

References

[1] K. Rajeshwar, *Advanced Materials*, 4, 23 (1992).

[2] R.N.Bhargava, *J. Crystal Growth*, 59, 15 (1982).

[3] W. Gebhart, *Materials Science and Engineering*, B11, 1 (1992).

[4] R.N. Bhargava, *J. Crystal Growth*, 117, 894 (1992).

[5] M. Neumann-Spallart and C. Konigstein, *Thin Solid Films*, 265, 33 (1995).

[6] K. Singh and J.P. Rai, *J. Mat. Sci. Lett.*, 4, 1401 (1985).

Figure 11: Graph of the coverage of the elements as a function of the number of ECALE cycles: (A) Zn (□) and S (△); (B) Zn (□) and Se (△); (C) Zn (□) and Te (△).

[7] C.B. Roy, D.K. Nandi, and P.K. Mahapatra, *Electrochim. Acta*, **31**, 1227 (1986).

[8] K. Singh and J.P. Rai, *Bull. Mater. Sci.*, **10**, 353 (1988).

[9] K. Singh and J.P. Rai, *Ind. J. Chem.*, **28A**, 557 (1989).

[10] J.P. Rai and K. Singh, *Ind. J. Chem.*, **32A**, 376 (1993).

[11] J.P. Rai, *Sol. Eng. Mat. Sol. Cells*, **30**, 119 (1993).

[12] I. Ohno, K. Wantanabe, and H. Numata, in *Electrochemically Deposited Thin Films*, M. Paunovic, I. Ohno, and Y. Miyoshi, Editors, **PV 93-26**, p.108, The Electrochemical Society Proceedings Series, Pennington, NJ (1993).

[13] K.Singh and R.K. Pathak, *Electrochim. Acta*, **39**, 2693 (1994).

[14] C. Natarajan, M. Sharon, C. Levy-Clement, M. Neumanne-Spallart, *Thin Solid Films*, **237**, 118 (1994).

[15] C.D. Lokhande, M.S. Jadhav, S.H. Pawar, *J. Electrochem. Soc.*, **136**, 2756 (1989).

[16] B.W. Sanders and A.H. Kitai, *J. Crystal Growth*, **100**, 405 (1990).

[17] T. Mahalingam and C. Sanjeeviraja, *Phys. Stat. Sol. (A)*, **129**, K89 (1992).

[18] B.W. Gregory, D.W. Suggs, and J.L. Stickney, *J. Electrochem. Soc.*, **138**, 1279 (1991).

[19] B.W. Gregory and J.L. Stickney, *J. Electroanal. Chem.*, **300**, 543 (1991).

[20] S. Bedair, *Atomic Layer Epitaxy*, Elsevier, Amsterdam, (1993).

[21] T.F. Kuech, P.D. Dapkus, Y. Aoyagi, Atomic Layer Growth and Processing, Materials Research Society, Pittsburg (1991).

[22] T. Suntola and J. Antson, U.S. Patent 4 058 430 (1977).

[23] D.M. Kolb in *Advances in Electrochemistry and Electrochemical Engineering*, Vol. 11, H. Gerischer and C.W. Tobias, Editors, Wiley, New York, 1978, p. 125.

[24] L.P. Colletti, R. Slaughter, and J.L. Stickney, J. Soc. Inform. Disp., submitted.

[25] L.P. Colletti and J.L. Stickney, in preparation.

[26] A.T. Hubbard, *Crit. Rev. Anal. Chem.*, **3**, 201 (1973).

[27] G. Adzic, J. McBreen, M.G. Chu, *J. Electrochem. Soc.*, **128**,1691 (1981).

[28] M.G. Chu, J. McBreen, G. Adzic, *J. Electrochem.Soc.*, **128**, 2281 (1981).

[29] A.R. Despic, and M.G. Pavlovic, *Electrochim. Acta*, **27**, 1539 (1982).[45] A. Nasar and M. Shamsuddin, *Thermochim. Acta*, **205**, 157 (1992).

[30] A. Tadjeddine and G. Tourillon, *Elektrokhimiya*, **29**, 63 (1993)

[31] M.A. Quaiyyum, A. Aramata, S. Moniwa, S. Taguchi, and M. Enyo, *J. Electroanal. Chem.*, **373**, 61 (1994).

[32] A. Aramata, M.A. Quaiyyum, W.A. Balais, T. Atoguchi, and M. Enyo, *J. Electroanal. Chem.*, **338**, 367 (1992).

[33] S. Taguchi, A. Aramata, M.A. Quaiyyum, and M. Enyo, *J. Electroanal. Chem.*, **374**, 275 (1994).

[34] S. Taguchi and A. Aramata, *J. Electroanal. Chem.*, **396**, 131 (1995).

[35] A.A. El-Shafei, *J. Electroanal. Chem.*, **380**, 269 (1995).

[36] J.W. Von Schultze, F.D. Koppitz, and M.M. Lohrengel, *Ber Bunsenges. Phys. Chem.*, **78**, 693 (1974).

[37] L.P. Colletti, D. Teklay, and J.L. Stickney, *J. Electroanal. Chem.*, **369**, 145, (1994).

[38] A. Hamelin, *J. Electroanal. Chem.*, **142**, 299 (1982).

[39] D.M. Kolb and J. Schneider, *Electrochim. Acta*, **31**, 929 (1986).

[40] J. Schneider and D.M. Kolb, *Surf. Sci.*, **193**, 579 (1988).

[41] X. Gao, A. Hamelin, and M.J. Weaver, *Phys. Rev. Lett.*, **67**, 618 (1991).

[42] A.N. Buckley, I.C. Hamilton, and R. Woods, *J. Electroanal. Chem.*, **216**, 213 (1987).

[43] I.C. Hamilton and R. Woods, *J. Appl. Electrochem.*, **13**, 783, (1983).

[44] X. Gao, Y. Zhang, and M.J. Weaver, *Langmuir*, **8**, 668 (1992).

[45] A. Nasar and M. Shamsuddin, *Thermochim. Acta*, **205**, 157 (1992).